Army Research Laboratory

Distance Traveled by a Hypervelocity Projectile in Air

by William P. Walters and Steven B. Segletes

ARL-TR-5612 July 2011

NOTICES

Disclaimers

Army Research Laboratory

Aberdeen Proving Ground, MD 21005-5066

ARL-TR-5612 **July 2011**

Distance Traveled by a Hypervelocity Projectile in Air

William P. Walters and Steven B. Segletes

Weapons and Materials Research Directorate, ARL

REPORT DOCUMENTATION PAGE			*Form Approved* *OMB No. 0704-0188*

1. REPORT DATE *(DD-MM-YYYY)*	July 2011
2. REPORT TYPE	Final
3. DATES COVERED (From - To)	April 2011-June 2011
4. TITLE AND SUBTITLE	Distance Traveled by a Hypervelocity Projectile in Air
5a. CONTRACT NUMBER	
5b. GRANT NUMBER	
5c. PROGRAM ELEMENT NUMBER	
6. AUTHOR(S)	William P. Walters Steven B. Segletes
5d. PROJECT NUMBER	AH80
5e. TASK NUMBER	
5f. WORK UNIT NUMBER	
7. PERFORMING ORGANIZATION NAME(S) AND ADDRESS(ES)	U.S. Army Research Laboratory ATTN: RDRL-WMP-C Aberdeen Proving Ground, MD 21005-5066
8. PERFORMING ORGANIZATION REPORT NUMBER	ARL-TR-5612
9. SPONSORING/MONITORING AGENCY NAME(S) AND ADDRESS(ES)	
10. SPONSOR/MONITOR'S ACRONYM(S)	
11. SPONSOR/MONITOR'S REPORT NUMBER(S)	
12. DISTRIBUTION/AVAILABILITY STATEMENT	Approved for public release; distribution is unlimited.
13. SUPPLEMENTARY NOTES	

14. ABSTRACT

An analytical study was conducted to determine the distance a high speed projectile, such as a shaped charge jet particle or a similar projectile, would travel in air when fired horizontally or vertically. The results are applicable to range safety when conducting tests with such devices.

15. SUBJECT TERMS

aerodynamic drag, range safety, particle trajectory

16. SECURITY CLASSIFICATION OF:			**17. LIMITATION OF ABSTRACT**	**18. NUMBER OF PAGES**	**19a. NAME OF RESPONSIBLE PERSON**
a. REPORT	**b. ABSTRACT**	**c. THIS PAGE**			Steven B. Segletes
Unclassified	Unclassified	Unclassified	UU	24	**19b. TELEPHONE NUMBER** (*Include area code*) 410-278-6010

Standard Form 298 (Rev. 8/98)
Prescribed by ANSI Std. Z39.18

Contents

List of Figures

List of Tables

INTENTIONALLY LEFT BLANK.

1. Introduction

Every introductory calculus student solves the problem of a projectile trajectory in a gravitational field for the case when there are no drag forces on the projectile. For that simplified case, the trajectory traces out a parabolic path in the atmosphere over time, while the horizontal component of velocity remains undiminished. In the real world, however, the projectile is subject to drag forces, which, at high Reynolds number, are estimated to be proportional to the square of the velocity. This drag force complicates the solution of the trajectory. Nonetheless, for certain special cases, an analytical solution by way of the calculus is still achievable.

An analytical study was conducted to determine the distance a hyper velocity projectile would travel in air. The projectile could be the tip particle of a shaped charge jet, an explosively formed penetrator, a bullet, or a similar device. Four cases were considered, namely, firing the projectile vertically upward, firing it horizontally under the restriction of "very small α" (where α is the time-dependent trajectory angle), firing it horizontally under a small α restriction, and finally, firing the projectile at a shallow trajectory (*i.e.*, a small positive or negative launch angle). The model is based on Newton's Law and the forces acting on the projectile are drag and gravity. Erosion, ablation, and strength of the projectile are not considered. This study is useful for experimental-range safety considerations and possibly jet-particle recovery.

2. Flight Retardation Equations

Consider a projectile of mass m (kg) launched at an initial velocity $V = V_0$ (m/s), at an angle α_0 with respect to the horizon, subject to the initial (time $t = 0$ s) conditions that the horizontal position $x = 0$ m, and with the vertical position y taking on a value of H, representing the height above ground (m) of the launch.

The velocity components at any given moment are given as

$$v_x = \dot{x} = V \cos \alpha \tag{1}$$

and

$$v_y = \dot{y} = V \sin \alpha \quad . \tag{2}$$

where α is the time-dependent trajectory angle with respect to the horizon, and the overdot denotes time differentiation. The aerodynamic drag force on the projectile is $\rho A C_d V^2/2$, where ρ is the density of air at sea level (1.293 kg/m^3), g is the acceleration due to gravity (9.806 m/s^2), C_d is the drag coefficient, and A is the effective cross-sectional area (m^2). The governing equations, accounting for the effects of aerodynamic drag and gravity and neglecting ablation, according to Newton's 2nd Law, are:

$$m\ddot{x} = -\frac{\rho A C_d V^2}{2} \cos\alpha \qquad = -\frac{\rho A C_d}{2}\dot{x}\sqrt{\dot{x}^2 + \dot{y}^2} \tag{3}$$

and

$$m\ddot{y} = -\frac{\rho A C_d V^2}{2} \sin\alpha - mg = -\frac{\rho A C_d}{2}\dot{y}\sqrt{\dot{x}^2 + \dot{y}^2} - mg \quad . \tag{4}$$

By lumping the term, $B = \rho A C_d/2m$, we may restate the governing set of equations as

$$\ddot{x} = -B\dot{x}\sqrt{\dot{x}^2 + \dot{y}^2} \tag{5}$$

$$\ddot{y} = -B\dot{y}\sqrt{\dot{x}^2 + \dot{y}^2} - g \quad . \tag{6}$$

The grouping within B, given by m/A, represents the areal density along the flight axis of the projectile, and may be alternately expressed as $\rho_p L_p$, where ρ_p is the projectile density and L_p is the characteristic length of the projectile. Thus, an alternative expression for B is given by $B = \rho C_d/2\rho_p L_p$.

We do not propose here to solve this full set of highly nonlinear governing equations for arbitrary launch angle α_0. However, we will use equations 5 and 6 to generate simplified governing equations for various special cases of the general problem.

---

3. The Vertical Model

For the case where the projectile is fired in the vertical direction, α remains at 90° throughout the projectile ascent. Equation 5 becomes trivial, and the governing equation 6 becomes

$$\ddot{y} = -(\rho A C_d/2m)\dot{y}^2 - g = -(B\dot{y}^2 + g) \quad , \tag{7}$$

From straightforward integration, references (*1–3*), we may obtain the vertical velocity $\dot{y}$ as a function of time t:

$$\dot{y}(t) = \sqrt{\frac{g}{B}} \tan\left[\sqrt{gB}\,(t_f - t)\right] \quad . \tag{8}$$

For this special case, the subscript f denotes the extremum condition when the projectile reaches maximum altitude. The time to reach the peak altitude is determined from equation 8 by the condition $\dot{y}(0) = V_0$:

$$t_f = \frac{1}{\sqrt{gB}} \tan^{-1}\left(V_0\sqrt{\frac{B}{g}}\right) \quad . \tag{9}$$

Assuming the projectile is launched from ground level, the altitude as a function of time is given as

$$y(t) = \frac{1}{B}\left\{\ln\cos\left[\sqrt{gB}\,(t_f - t)\right] - \ln\cos\left(\sqrt{gB}\,t_f\right)\right\} \quad . \tag{10}$$

The projectile's peak altitude, which is reached at $t = t_f$, is therefore

$$y_f = -\frac{1}{B}\left\{\ln\cos\left(\sqrt{gB}\,t_f\right)\right\} \quad . \tag{11}$$

Upon the projectile's return trip to the ground, the sense of y (and thus $\dot{y}$ and $\ddot{y}$) is reversed in equation 7. The terminal velocity of the downward falling projectile is achieved when $\ddot{y} = 0$. This condition allows for the well-known algebraic solution for the terminal velocity as

$$\dot{y}_{\text{term}} = \sqrt{\frac{2mg}{\rho A C_d}} = \sqrt{g/B} \quad . \tag{12}$$

---

4. The "Very Small α" Horizontal-Launch Model

Consider a projectile fired parallel to the x-axis as another special case of the governing equations, where the initial height $y(0) = H$ of the launch is very small, such that, over the duration of the flight, the vertical velocity $\dot{y}$ and, thus, the angle of attack α remain *very* small. Specifically, we require constraints that both $\dot{y} \ll \dot{x}$ and $BV^2 \sin\alpha \ll g$. Under the first constraint, the velocity $V = \sqrt{\dot{x}^2 + \dot{y}^2}$ may be approximated as $\dot{x}$. Employing this approximation, the second constraint may be restated as $B\dot{x}\dot{y} \ll g$, which effectively discards the first term on the right-hand side of equation 6 (the vertical component of aerodynamic drag) as insignificant relative to the second term (gravity g).

For this simplified case, in which the vertical component of aerodynamic drag is insignificant with respect to the projectile weight, the governing equations (equations 5 and 6) become

$$\ddot{x} = -B\dot{x}^2 \tag{13}$$

$$\ddot{y} = -g \quad . \tag{14}$$

From equation 14, $\dot{y} = -gt$ and

$$y = -gt^2/2 + H \quad . \tag{15}$$

Here, we denote the terminal condition with a subscript f when the projectile reaches the ground (*i.e.*, the x-axis), we have, as $y \to 0$, that

$$t_f = \sqrt{2H/g} \quad . \tag{16}$$

In the x direction, we may integrate equation 13 once to obtain

$$\dot{x} = V_0/(BV_0t + 1) \quad . \tag{17}$$

Separate the variables and integrate again:

$$x = \ln[BV_0t + 1]/B \quad . \tag{18}$$

Finally, as $y \to 0$ at $t = t_f$ from equation 16, we obtain the velocity as $\dot{x}_f = V_0/(BV_0\sqrt{2H/g} + 1)$ and the position as

$$x_f = \ln[BV_0\sqrt{2H/g} + 1]/B \quad . \tag{19}$$

The term x_f represents the horizontal distance the projectile is anticipated to travel prior to reaching the ground. As it reaches the ground, its horizontal velocity is not zero, but will be given by equation 17 evaluated at $t = t_f$.

5. The Small α Horizontal-Launch Model

While the "very small α" horizontal-launch model allows for a closed-form solution of all terms, it is overly restrictive to assume that the vertical component of aerodynamic drag force is negligible relative to the projectile weight. As the projectile velocity becomes hypersonic, this restrictive assumption becomes even less applicable. A more general solution to the governing equations 5 and 6 may be obtained by relaxing this constraint.

With this revised approach, we still assume a small-angle constraint, $\alpha \approx 0$, which is equivalent to $\dot{y} \ll \dot{x}$. However, we enforce no restrictions on the magnitude of the drag force relative to the projectile weight. In this revised approach to the horizontal-launch model, the governing equations become

$$\ddot{x} = -B\dot{x}^2 \tag{20}$$

$$\ddot{y} = -B\dot{x}\dot{y} - g \quad . \tag{21}$$

Equation 20 is the same as equation 13, which, in turn, will lead to the same results for $\dot{x}$ and x, governing the horizontal motion of the projectile. Thus, equations 17 and 18 likewise apply to this more general horizontal-launch model, which we restate here for convenience:

$$\dot{x} = V_0/(BV_0 t + 1) \tag{22}$$

$$x = \ln[BV_0 t + 1]/B \quad . \tag{23}$$

Turning to the equation 21, we use the chain rule to express $\ddot{y}$ as $d\dot{y}/dx \cdot dx/dt$, or $\dot{x}\ d\dot{y}/dx$. This equation may then be re-expressed as

$$\frac{d\dot{y}}{dx} + B\dot{y} = -\frac{g}{\dot{x}} \quad . \tag{24}$$

However, from equations 22 and 23, we observe that $1/\dot{x} = e^{Bx}/V_0$. Thus, substituting into equation 24,

$$\frac{d\dot{y}}{dx} + B\dot{y} = -\frac{g}{V_0}\, e^{Bx} \quad . \tag{25}$$

While equation 25 reveals that $\dot{y}$ will clearly be exponential in x, it must also satisfy the initial horizontal-launch condition that $\dot{y} = 0$ at $t = 0$ (which also coincides with $x = 0$).

A solution is found in the expression

$$\dot{y} = -\frac{g}{BV_0}\sinh(Bx) \quad . \tag{26}$$

Since $e^{Bx} = BV_0t + 1$, equation 26 may be integrated again for y, as

$$y = \frac{gx}{2BV_0^2} - \frac{gt^2}{4} - \frac{gt}{2BV_0} + H \quad . \tag{27}$$

Note that the term x has been used to replace a logarithmic expression, which arises in the integration, $\ln(BV_0t+1)/B$, in equation 27. A Taylor expansion of this first term of equation 27 can be shown (to three terms) to be

$$\frac{gx}{2BV_0^2} = \frac{g}{2B^2V_0^2}\ln(BV_0t+1) = 0 + \frac{gt}{2BV_0} - \frac{gt^2}{4} + \ldots \qquad (-1 < BV_0t \leq 1) \quad . \tag{28}$$

If only the first three terms of the expansion are taken, then equation 27 becomes $y = -gt^2/2 + H$, which is precisely the "very small α" horizontal-launch model of section 4. Seeing that the "very small α" model uses only three expansion terms of the more accurate logarithmic form and that it can be inadvertently applied when $BV_0t > 1$, outside the zone of convergence, provides additional emphasis on just how limited the "very small α" model is in its utility. In contrast, the logarithmic form of x, as part of the full solution given by equation 27, plays a significant role at later values of t, as the projectile travels downrange (*i.e.*, at larger x).

Unlike the "very small α" horizontal-launch model of section 4, we cannot solve, in closed form, for the time, t_f, at which the projectile strikes the ground (*i.e.*, when $y = 0$). However, a rapidly converging iteration may be set up to obtain t_f. Start with $x = 0$ and quadratically solve equation 27 for a trial value of t for which $y = 0$. This trial value of time may be substituted into equation 23 to obtain an updated value of projectile travel distance x. The updated value of x may be employed as the iteration alternately employs equation 27 and equation 23. Convergence is achieved rapidly, because of the logarithmic response of equation 23 is relatively insensitive to large changes in x.

6. The Shallow-Trajectory Model

We consider now the case where the projectile is fired essentially in the horizontal direction, except for a slight perturbation in the initial elevation angle at launch, α_0, such that $\alpha_0 \ll 1$. Because α remains small, we retain the "small α" assumption ($\cos\alpha \approx 1$, $\sin\alpha \approx \alpha$) and thus the simplifications to the governing equations employed for the small α horizontal-launch model, as given by equations 20 and 21.

Therefore, the solution to equation 20 remains unchanged, and the expressions given in equations 22 and 23 remain in force for the shallow-trajectory model. The difference between this case and the small α horizontal-launch model is in the initial condition on $\dot{y}$. Whereas $\dot{y}(0) = 0$ identically in the horizontal-launch case, here we have

$$\dot{y}(0) = V_0 \sin\alpha_0 \approx V_0\alpha_0 \quad . \tag{29}$$

The solution, in this case, is generalized from the approach of section 5 and amounts to resolving equation 25 under a different initial condition. The solution is given as

$$\dot{y} = -\frac{ge^{-\gamma}}{BV_0}\sinh(Bx - \gamma) \quad , \tag{30}$$

where

$$\gamma = \frac{1}{2}\ln\left(1 + \frac{2BV_0^2\alpha_0}{g}\right) \quad . \tag{31}$$

When α_0 is zero, $\gamma = 0$ and equation 30 returns to the horizontal-launch form of equation 26.

With $\dot{y}$ known through equation 30, the angle of attack α may also be expressed. It is given as

$$\tan\alpha = \frac{\dot{y}}{\dot{x}} = \frac{g}{2BV_0^2}\left(e^{2\gamma} - e^{2Bx}\right) \quad . \tag{32}$$

Knowledge of α can be used to gauge when the governing constraint of the "small α" assumption no longer applies.

Likewise, equation 30 may be integrated to obtain y as

$$y = \left(\frac{g}{2BV_0^2} + \alpha_0\right)x - \frac{gt^2}{4} - \frac{gt}{2BV_0} + H \quad . \tag{33}$$

Analogous to the small α horizontal-launch model, the solution for impact time t_f in the shallow-trajectory model may be obtained through iteration of t and x, by initially assuming $x_f = 0$. This technique will converge when $(g/2BV_o^2 + \alpha_0)$ is nonnegative. The form of equation 33 that quadratically solves for t when $y = 0$ is given by

$$t_f = -\frac{1}{BV_0} + \sqrt{\left(\frac{1}{BV_0}\right)^2 + \frac{4}{g}\left[H + \left(\frac{g}{2BV_0^2} + \alpha_0\right) x_f\right]} \quad . \tag{34}$$

Thus, the iteration is performed on equations 34 and

$$x_f = \ln[BV_0 t_f + 1]/B \tag{35}$$

to obtain t_f and x_f, respectively (since the projectile range will be obtained as $x_f = x(t_f)$ through equation 23). For all the equations presented in this section, when $\alpha_0 = 0$, the small α horizontal-launch model is recovered.

For negative-α_0 cases where $(g/2BV_o^2 + \alpha_0)$ is negative, other techniques may be used to solve for x_f and t_f if the iteration described above fails. For example, t may be progressively advanced by small increments, with the corresponding x being calculated via equation 23. These incremental values for t and x may be substituted into equation 33 until such time is reached where y becomes negative. A suitably small time increment may be used to achieve the desired resolution. The values of t and x when y changes sign are, in fact, t_f and x_f, respectively.

7. Computational Results

The cases studied in this section are based on reported drag coefficients for various shaped-charge jet particles (*4*) or else constitute particles of a hypothetical construct. In all cases, the particles considered are projected in air at or near the surface of the Earth. While cases 1 through 4 are based on the experimental data of Chou *et al.* (*4*), case 5 is hypothetically constructed as a representative explosively formed penetrator (EFP) particle.

Results for the vertical-launch model are given in table 1. The particulate projectiles are imagined to have been launched vertically from the surface of the Earth (Note: the drag coefficients are based on the given "particle profile" figures, as if flying from left to right across the page). The third column of the table denotes the particles' areal density along their flight axis. It can be obtained as mass per unit cross-sectional area or alternately as projectile density times effective length, depending on which data were measured/estimated. In the table, the columns y_f and t_f, respectively, indicate the maximum altitude reached by the particle, and the time to reach that altitude. The $\dot{y}_{\text{term}}$ column indicates the maximum (terminal) velocity with which the particle returns back to the Earth's surface.

Table 1. Cases studied using the vertical model (section 3).

Case	V_0 (m/s)	$m/A = \rho_p L_p$ (kg/m^2)	C_d	B (m^{-1})	Liner Shape	Particle Profile	y_f (m)	t_f (s)	$\dot{y}_{\text{term}}$ (m/s)
1	4650	27.0	0.68	0.0163	38 mm hemi		321.8	3.9	24.5
2	4250	156.8	2.11	0.0087	127 mm hemi		556.3	5.4	33.6
3	4230	146.3	2.31	0.0102	127 mm hemi(P)	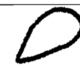	481.5	4.9	31.0
4	7670	88.2	2.29	0.0168	81.3 mm cone		343.1	3.9	24.2
5	2000	445.0	1.00	0.00145	Hypothetical EFP		2197.9	13.	82.2

Results for the "very small α" horizontal-launch model are given in table 2 and may be compared to those results for the small α horizontal-launch model, given in table 3. The parameter B is constructed, in part, using the areal density along the flight axis of the projectile. The axial areal density can be given as either m/A or $\rho_p L_p$, which accounts for the two formulae for calculating B, as mentioned in section 2. This also accounts for why cases 1–4 provide m and A, whereas case 5 provides L_p and ρ_p.

Table 2. Cases studied using the "very small α" horizontal-launch model (section 4).

Case	H (m)	V_0 (m/s)	A (m^2)	m (kg)	C_d	B (m^{-1})	Liner Shape (P=Precision)	Particle Profile	x_f (m)	t_f (s)
1	1	4650	0.152×10^{-4}	0.00041	0.68	0.0163	38.1 mm hemi	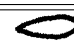	218.5	0.45
2	1	4250	1.094×10^{-4}	0.01715	2.11	0.0087	127 mm hemi		330.2	0.45
3	1	4230	1.150×10^{-4}	0.01682	2.31	0.0102	127 mm hemi(P)	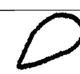	295.8	0.45
4	1	7670	0.322×10^{-4}	0.00284	2.29	0.0168	81.3 mm cone	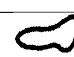	243.1	0.45
			L_p (m)	ρ_p (kg/m^3)						
5	1	2000	0.05	8900	1.0	0.00145	Hypothetical EFP		577.0	0.45

Table 3. Cases studied using the small α horizontal-launch model (section 5).

Case	H (m)	V_0 (m/s)	A (m^2)	m (kg)	C_d	B (m^{-1})	Liner Shape (P=Precision)	Particle Profile	x_f (m)	t_f (s)
1	1	4650	0.152×10^{-4}	0.00041	0.68	0.0163	38.1 mm hemi	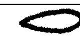	238.2	0.63
2	1	4250	1.094×10^{-4}	0.01715	2.11	0.0087	127 mm hemi	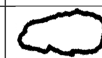	364.1	0.62
3	1	4230	1.150×10^{-4}	0.01682	2.31	0.0102	127 mm hemi(P)	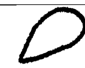	325.4	0.62
4	1	7670	0.322×10^{-4}	0.00284	2.29	0.0168	81.3 mm cone	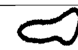	262.7	0.63
			L_p (m)	ρ_p (kg/m^3)						
5	1	2000	0.05	8900	1.0	0.00145	Hypothetical EFP		632.4	0.52

For all horizontal cases studied here, the particles were imagined to have been launched (horizontally) from an elevation of 1 m above the Earth. For the particles whose characteristics were drawn from Chou *et al.* (*4*), the shape of the particle (as projected upon an x-ray) is shown in the "Particle Profile" column. As before, the orientation of the particle used to calculate the drag coefficient assumes the given particle shapes are travelling across the page from left to right. The column listed as x_f shows the predicted travel range of the particle, while the t_f column gives the time at which the particle impacts the Earth's surface. In the "very small α" horizontal-launch model, all impact times are identical at 0.45 s, because they are all launched at 1 m of altitude and, in the vertical direction, are subject only to downward gravitational forces. The more general small α horizontal-launch model reveals longer times and larger distances traveled, by comparison. This extension of the flight duration is because the downward motion of the particle towards the Earth is retarded by a component of the particle's drag force.

Finally, the case of shallow trajectory was studied for these five cases. Initial launch angle (α_0) was varied from $-0.5°$ to $2°$, and the resulting horizontal travel range was calculated. The results are presented in figure 1, for the five particles already studied. For positive launch elevations, the range increases rapidly as elevation increases. However, the range eventually flattens out, with increasing elevation, in a manner more severe than would be expected from a drag-free parabolic trajectory. In essence, the range is being saturated as a result of horizontal deceleration rate, despite the additional vertical boost provided by an increase in elevation angle. Nonetheless, for particles with a high length-to-diameter ratio, which remain aerodynamically stable in flight (for example, case 5), drag plays a lesser role in the projectile's flight. In such cases, travel range can be significantly increased by even small changes in the initial elevation angle.

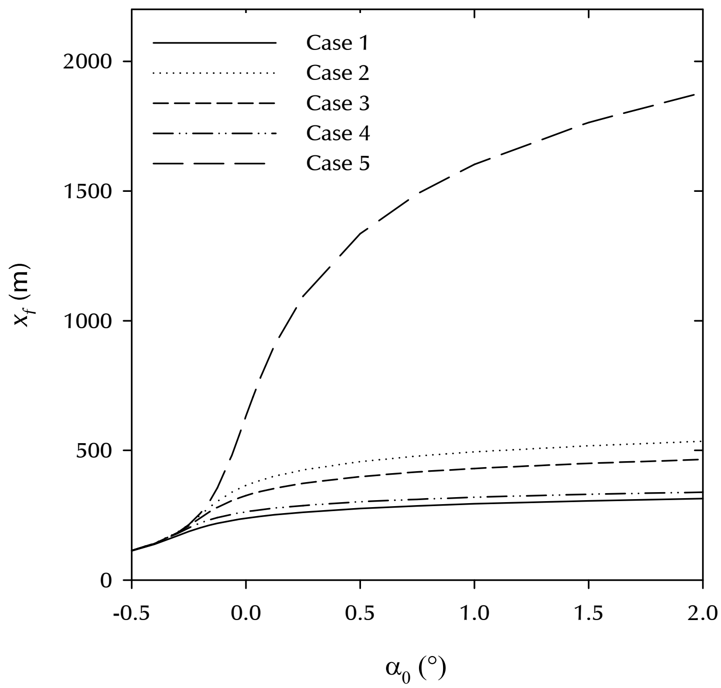

Figure 1. Influence of small elevation angle upon projectile range for projectiles fired from 1 m in elevation.

The figure also shows the effect of negative launch elevation, down to $-0.5°$. As launch elevation becomes more negative, all cases converge toward the same curve. Such behavior is also expected, since for negative elevations, the range is increasingly determined by launch orientation and less by drag. In the limit, for high-speed launches at negative elevation, the range will approach $x_f \to H \cot(-\alpha_0)$. This result is independent of the specific characteristics of particle geometry, drag, *etc.*, and will depend upon only the initial launch height H and the launch angle α_0, if the launch velocity is sufficiently large to overwhelm the effects of gravity.

8. Summary and Conclusions

It is of interest to know how far a jet particle from a shaped charge or similar device will travel if fired into air. This interest stems from the fact that some test ranges are located near bodies of water, highways, or structures and the possibility exists that the projectile may miss or perforate the intended target. Toward this end, models were constructed to predict projectile travel in a horizontal, vertical, or shallow angle trajectory based on the measured particle characteristics and calculated drag coefficients from Chou *et al.* (*4*). For the five particular cases studied, a projectile could travel from 320 to 2200 m in the vertical direction with a terminal velocity of 24 to 82 m/s. Under horizontal launch, according to the small α model, the projectile could travel from 238 to 632 m in the horizontal direction. Using the less accurate "very small α" model, the estimated ranges are 217 to 577 m, which, for the test cases studied, is about a 10% underprediction as compared to the more accurate small α model. When the shallow-trajectory model was employed, these same test cases studied could travel from 314 to 1880 m for shallow launch trajectories of 2°.

9. References

1. Walters, W.; Summers, R.; Segletes, S. *Soft Recovery of a Ballistic Projectile*; ARL-TR-2034; U.S. Army Research Laboratory: Aberdeen Proving Ground, MD, August 1999.

2. Segletes, S. B.; Walters, W. P. Extensions to the Exact Solution of the Long-Rod Penetration/Erosion Equations. *International Journal of Impact Engineering* **2003**, *28*, 363–376.

3. Segletes, S. B. *Modeling the Penetration Behavior of Rigid Spheres into Ballistic Gelatin*; ARL-TR-4393; U.S. Army Research Laboratory: Aberdeen Proving Ground, MD, March 2008.

4. Chou, P. C.; Ciccarelli, R. D.; Walters, W. P. *The Virtual Origin and Tip Particle Drag Coefficient of Shaped Charge Jets*; ARBRL-CR-00522; U.S. Army Ballistic Research Laboratory: Aberdeen Proving Ground, MD, January 1984.

NO. OF COPIES	ORGANIZATION
1 (PDF ONLY)	DEFENSE TECHNICAL INFORMATION CTR DTIC OCA 8725 JOHN J KINGMAN RD STE 0944 FORT BELVOIR VA 22060-6218
1	DIRECTOR US ARMY RESEARCH LAB IMNE ALC HRR 2800 POWDER MILL RD ADELPHI MD 20783-1197
1	DIRECTOR US ARMY RESEARCH LAB RDRL CIO LL 2800 POWDER MILL RD ADELPHI MD 20783-1197
1	DIRECTOR US ARMY RESEARCH LAB RDRL CIO MT 2800 POWDER MILL RD ADELPHI MD 20783-1197
1	DIRECTOR US ARMY RESEARCH LAB RDRL D 2800 POWDER MILL RD ADELPHI MD 20783-1197

NO. OF COPIES	ORGANIZATION
1	AIR FORCE ARMAMENT LAB AFATL DLJR D LAMBERT EGLIN AFB FL 32542-6810
3	COMMANDER US ARMY ARDEC AMSTA AR WEE C E BAKER A DANIELS R FONG B3022 PICATINNY ARSENAL NJ 07806-5000
2	COMMANDER US ARMY AVN & MISSILE CMD AMSAM RD PS WF S CORNELIUS S HOWARD REDSTONE ARSENAL AL 35898-5247
2	DARPA W SNOWDEN S WAX 3701 N FAIRFAX DR ARLINGTON VA 22203-1714
9	LLNL ROBERT E TIPTON L-095 DENNIS BAUM L-163 MICHAEL MURPHY L-099 TOM MCABEE L-095 GLENN POMYKAL L-072 JOHN E REAUGH L-282 ROBERT M KUKLO L-099 G SIMONSON L-099 R BARKER L-020 PO BOX 808 LIVERMORE CA 94550
5	LOS ALAMOS NATL LABORATORY L HULL MS A133 C WINGATE MS D413 C RAGAN MS D449 E J CHAPYAK MS F664 J BOLSTAD MS G787 PO BOX 1663 LOS ALAMOS NM 87545

NO. OF COPIES	ORGANIZATION
3	SOUTHWEST RSRCH INST C ANDERSON S A MULLIN J WALKER PO DRAWER 28510 SAN ANTONIO TX 78228-0510
3	DE TECHNOLOGIES R CICCARELLI W FLIS W CLARK 100 QUEENS DR KING OF PRUSSIA PA 19406
1	TEXTRON DEFNS SYS C MILLER 201 LOWELL ST WILMINGTON MA 01887-4113
1	LOCKHEED MARTIN ELECT & MIS G W BROOKS 5600 SAND LAKE RD MP 544 ORLANDO FL 32819-8907
1	GD OTS J OSBORN 4565 COMMERCIAL DR A NICEVILLE FL 32578
2	GD OTS D BOEKA N OUYE 2950 MERCED ST STE 131 SAN LEANDRO CA 94577
1	JAMS PROJECT OFFICE ATTN: SFAE-MSLS-JAMS-SYS-O C ALLEN 5250 MARTIN RD REDSTONE ARSENAL AL 35898
1	HALLIBURTON ENERGY SVCS JET RESEARCH CTR D LEIDEL PO BOX 327 ALVARADO TX 76009-9775
1	NORTHROP GRUMMAN DR D PILLASCH B57 D3700 PO BOX 296 1100 W HOLLYVALE ST AZUSA CA 91702

NO. OF COPIES	ORGANIZATION
1	INTRNTL RSRCH ASSOC D ORPHAL 4450 BLACK AVE PLEASANTON CA 94566-6105
	ABERDEEN PROVING GROUND
67	DIR USARL RDRL SL P TANENBAUM RDRL SLB R BOWEN RDRL SLB D R GROTE L MOSS J POLESNE RDRL SLB E M PERRY C BARKER D FORDYCE P HORTON D HOWLE D LYNCH M MAHAFFEY R SAUCIER RDRL SLB G P MERGLER RDRL SLB S R BOWERS M OMALLEY RDRL SLB W L ROACH J ABELL W MERMAGEN RDRL WM P PLOSTINS RDRL WMS T ROSENBERGER RDRL WML M ZOLTOSKI RDRL WML C K MCNESBY RDRL WML H T EHLERS T FARRAND E KENNEDY L MAGNESS C MEYER B SORENSEN R SUMMERS RDRL WMM B G GAZONAS RDRL WMP P BAKER S SCHOENFELD RDRL WMP B C HOPPEL S R BILYK D CASEM M GREENFIELD C WILLIAMS RDRL WMP C T BJERKE J BARB N BRUCHEY T DIGLIANI R MUDD S SEGLETES (5 COPIES) W WALTERS (5 COPIES) RDRL WMP D J RUNYEON R FREY D KLEPONIS H W MEYER B SCOTT K STOFFEL RDRL WMP E M BURKINS W A GOOCH E HORWATH B LOVE RDRL WMP F N GNIAZDOWSKI E FIORAVANTE RDRL WMP G N ELDREDGE S KUKUCK